

## **DETECTION AND LOCALISATION OF BARELY VISIBLE IMPACT DAMAGE IN FIBRE-REINFORCED POLYMER COMPOSITES USING A SUPERVISED DEEP LEARNING ALGORITHM**

Ali Tabatabaeian, University of Glasgow, UK, 2611578T@student.gla.ac.uk

Bruno Jerkovic, Radboud University, Netherlands, bruno.jerkovic@ru.nl

Felipe Vannucchi de Camargo, SENAI Institute of Innovation in Polymer Engineering, Brazil, felipe.camargo@senairs.org.br

Leonel Echer, SENAI Institute of Innovation in Polymer Engineering, leonel.echer@senairs.org.br

Elena Marchiori, Radboud University, Netherlands, e.marchiori@cs.ru.nl

Mohammad Fotouhi, Delft University of Technology, Netherlands, m.fotouhi-1@tudelft.nl

### **ABSTRACT**

Composites are prone to internal damage, either during manufacture or throughout their service life, requiring non-destructive testing for detection, monitoring, and repair. However, some methods, such as visual inspection, may pose health and safety risks. The present work explores the use of a supervised deep-learning algorithm to identify barely visible impact damage in composite panels. The algorithm is trained on a small labelled dataset and tested on an unlabelled dataset. Results show that the algorithm could present a promising tool for automating structural health monitoring of composites, offering accuracy of 96% and 86% on the non-impacted and impacted surfaces.

### **KEYWORDS**

Structural health monitoring (SHM); Barely visible impact damage (BVID); Deep learning.

### **INTRODUCTION**

Artificial Intelligence (AI) based methodologies for detecting impact-induced damage in Fibre Reinforced Polymer (FRP) composite structures fall into either of these primary methods: (i) image-based methods, (ii) vibration-based methods, and (iii) acoustic-based methods. Image-based methods utilise computer vision algorithms to scrutinise images of the surface of composite panels both before and after an impact event. This technique detects any changes in surface topography, such as cracks and fibre breaks. Vibration-based methods, on the other hand, focus on measuring and analysing the vibrational response of the FRP composite structure to detect any changes in mechanical properties, including stiffness and damping, caused by impact damage. Acoustic-based methods utilise acoustic sensors to detect any changes in the Acoustic Emission (AE) signals produced by impact damage.

Numerous studies have explored the application of AI-based methods to detect, quantify and classify impact damage in composite materials (Ahmed et al., 2021). For instance, Zargar & Yuan (2021) demonstrated that it is possible to utilise a Deep Learning (DL) model to characterise impact damage by studying the evolution of the propagating waves generated by an impact. They embedded the physics of wave propagation into the model's architecture, making it a physics-inspired DL model rather than just a data-driven one. Fotouhi et al. (2021) suggested the utilisation of DL to quantitatively assess the visual detection of common microscale damages, such as matrix cracking and fibre breakage, in composite structures. They successfully demonstrated that DL could automate visual inspection and highlighted the need for an improved dataset library and custom classifiers for DL training. Wei et al. (2021) employed infrared thermography data of impacted curved Carbon Fibre Reinforced Polymer (CFRP) composites to train two different DL models. Both models were able to identify impact damage and predict the damaged location with an F1-score of 92.74% on mid-wave infrared data and an F1-score of 87.39% on long-wave infrared data. Hasebe et al. (2022) utilised three Machine Learning (ML) models on a dataset extracted from Low-Velocity Impact (LVI) tests on composites, with particular attention given to three influential factors: stacking sequence, impactor

shape, and impact energy. Their findings indicated that local volume, the gradient of the dent surface, and the pure dent depth could be used to characterise internal damage in CFRP laminates.

In most of the studies reviewed here, collecting a dataset needs advanced knowledge and measurement facilities such as Pulsed Thermography equipment (K. Deng et al., 2023), 3D measurement systems for evaluating impact dent depth (Hasebe et al., 2022b, 2022a), or signal processing to convert impact signals into input image data (Jung et al., 2021). An improvement of this work over other research in the literature is the successful implementation of a ResNet to predict the Barely Visible Impact Damage (BVID) only from very simple surface images. The results section discusses the model's accuracy on the top face (impacted side) and back face (non-impacted side).

## EXPERIMENTAL PROCEDURE

CFRP samples were manufactured applying the hand lay-up technique, where 32 plies of T800 carbon prepregs were laid up with the  $[45/0/90/-45]_{4s}$  configuration and cured according to the supplier's instructions. All samples were manufactured according to ASTM-D7136 for impact tests of composite materials (Fotouhi et al., 2021).

Quasi-static indentation tests (see Figure 1) were first used to understand the behaviour of the investigated samples and to choose appropriate energy levels for the impact tests, as described in Fotouhi et al. (2021). LVI tests with different energy levels, from 3J to 128J, were then carried out using an Instron Dynatup 9250 HV drop weight impact tower and according to the ASTM D7136 standard (Fotouhi et al., 2021). The impact load and deflection were measured by a single accelerometer inside the tup, and the measured data was processed by a 4kHz filter of the console software to reduce the noise and oscillations.

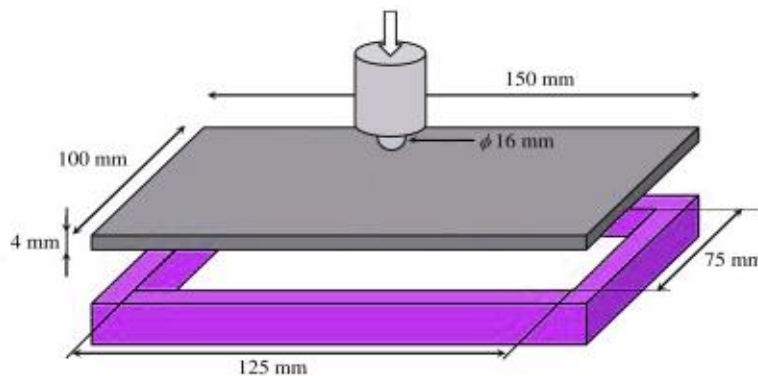


Figure 1: A schematic of indentation and impact tests apparatus.

After completing LVI tests, two Non-Destructive Evaluation (NDE) methods, including C-scan and visual inspection were conducted. In the first approach, a 10 MHz transducer was used to scan the samples in a water tank. USL Software was used to adjust the scanning parameters. The damage area was measured in the software and the results were then recorded. In the second approach, a Nikon camera was used to take an image of the front-face and back-face of all samples. Accordingly, a detailed internal and surface damage dataset was collected.

## DEEP LEARNING MODEL

A pre-trained Residual Network (ResNet) architecture with 18 trainable layers was used in this paper. ResNet is a deep neural network architecture to address the problem of vanishing gradients in very deep CNNs. It allows for the training of deep networks with hundreds of layers by introducing shortcut connections between the layers, which skip over certain layers and allow the network to learn residual functions. ResNet architecture's advantages over simple CNNs include training deeper networks and achieving higher accuracy with faster training time. Figure 2(a) shows a residual block. Another advantage of ResNet is that it is possible to start the training with the values of its weights learned from a different task or dataset (transfer learning). For example, ImageNet (J. Deng et al.,

2009) is a large-scale image database containing over 14 million images, widely used for training and evaluating computer vision models. Here, ResNet 18 – available from Pytorch (Paszke et al., 2019) – was pre-trained on more than a million images from the ImageNet database. Even though there are available pre-trained ResNet architectures with even more layers, because of the small size of our dataset, we did not use a bigger architecture, so that it does not overfit the data. However, we have replaced its last fully connected layer with a new one that outputs only one number. After that, we put a Sigmoid activation function to turn it between 0 and 1, so that we could use it as a probability of the input image either being damaged or not. Furthermore, Adam was used as an optimiser, and the Binary Cross Entropy (BCE) as a loss function. The model is first trained and validated using only a small part of a labelled dataset. Then, it is tested on an unlabelled dataset. When the model sees the entire training set, it is called one epoch of the model. The point that early stopping stops the model from training is the point where the validation loss starts increasing. Figure 2(b) shows an example of the loss with respect to the number of epochs.

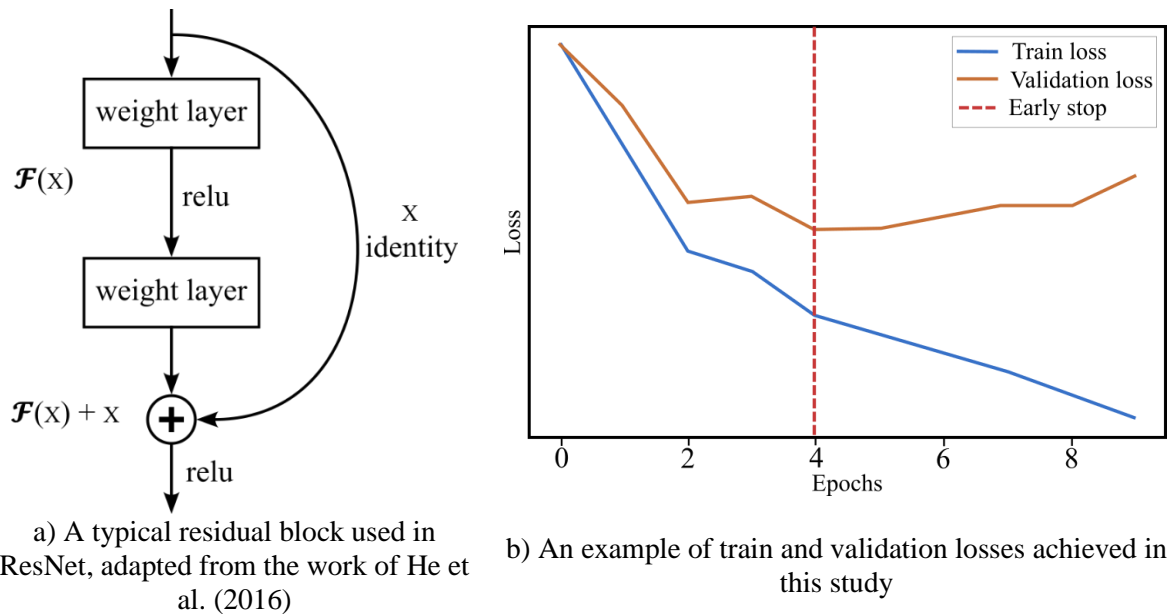


Figure 2: Deep learning model used in this study

## RESULTS

### LVI and NDE results

The results of LVI tests are shown in Figures 3 and 4. As seen in Figure 4(a), except for 3J and 6J, a significant load drop can be seen in all energy levels associated with delamination initiation. Low energy levels (3J and 6J) do not cause any damage to the samples; therefore, there is no load drop for these energies. In Figure 4(b), a considerable load drop occurred in 96J and 128J due to fibre failure. In these impact energies, there is a significant residual deflection. Energy absorption in composite structures under impact load can cause various damage mechanisms. Therefore, damage mechanisms can be characterised by analysing energy absorption. As shown in Figure 3, there is a significant change in the absorbed energy-time response of specimens, where energy absorption for impact energies lower than 64J is almost half of those higher than 64J. This is in line with the results of Figure 4, suggesting that a specific range of energy from 8J to 64J is of great importance as the damage mechanism in this energy range is delamination, which causes BVID.

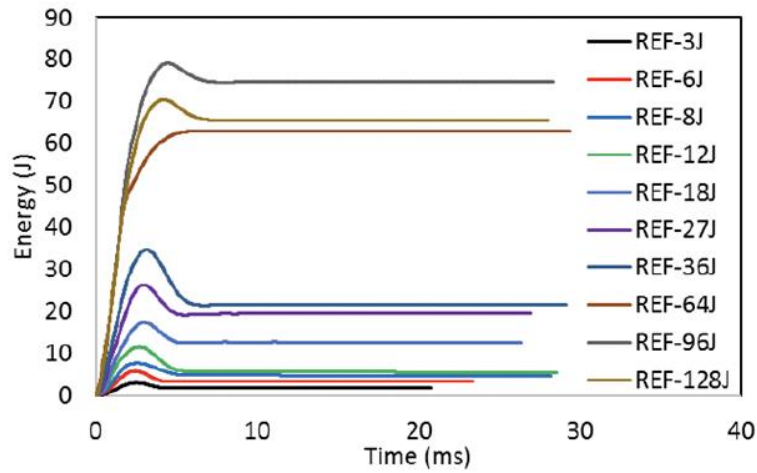
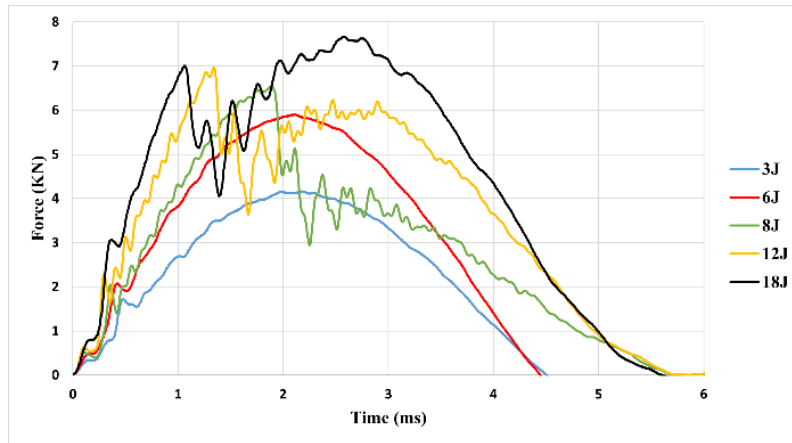
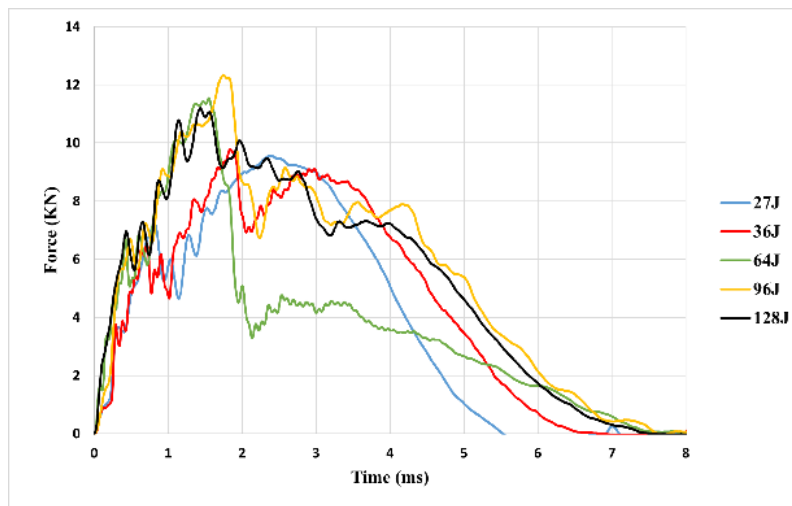


Figure 3: LVI test results: energy absorption-time response



a) Energy range from 3J to 18J.



b) Energy range from 27J to 128J.

Figure 4: LVI test results for the force-time response.

Figure 5 shows the C-scan, front-face, and back-face images of the CFRP samples. The c-scan images show no internal damage associated with 3J and 6J impact energies, and delamination starts from 8J. It is also indicated that damage size varies in line with impact energy. Images of the front-face and

back-face of samples clarify that damage is visible only at the energy levels of 96J and 128J, barely visible at 12J-64J, and invisible at 8J. These images suggest that the back-face may allow for better damage visibility than the front-face, particularly for higher energy levels such as 64J, 96J, and 128J

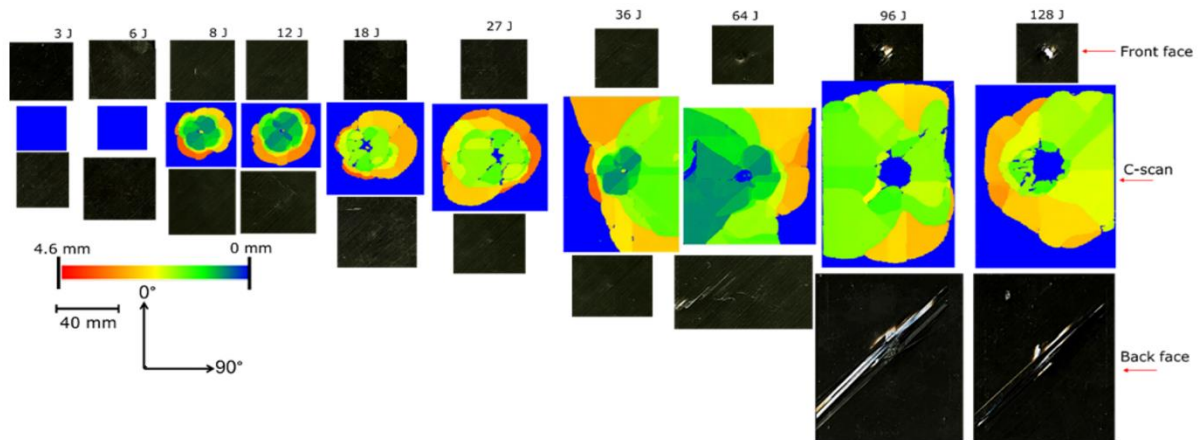


Figure 5: Front-face, back-face, and C-scan images of reference samples at different impact energies.

### BVID Detection using ResNet

Based on the previous section results, images of front-face and back-face of samples impacted at 12J-64J are used as input to the DL model. Accordingly, two different datasets (tasks) are defined as presented in Table 1.

Table 1: Classification of the dataset

Task number (dataset)	Type of composite panel	Damage location	Damage range
1	32-ply	back-face	within the BVID range
2	32-ply	front-face	within the BVID range

The results of the BVID detection using the ResNet are presented here. All evaluation parameters presented in Table 2 show that it is easier for the model to detect the damage on back-face than front-face. For example, the accuracy of damage prediction on back-face is nearly 10% higher than on the front-face. This can be due to different visible or barely visible damage patterns developed during the impact event on the two sides. This aligns with the visual observation results, as damage on the back-face is more visible than the front-face. Note that here, we only use images of samples damaged within the BVID energy range, and different results may be achieved if images of higher impact energies are used as input to the model. The results presented in Table 3 indicate that the difference between the training time for the back-face and front-face is not very significant.

In the case of damage detection across an image dataset when using a DL model, four outcomes can be expected to achieve: True Positives (TP), True Negatives (TN), False Positives (FP), and False Negatives (FN), which are defined as follows:

TP: The number of images that the network has correctly identified as containing the damage.

TN: The number of correctly identified undamaged images.

FP: The number of undamaged images that are incorrectly identified as damaged images.

FN: The number of damaged images that the network has incorrectly identified as undamaged images.

It is noticeable on the FP images that there are prevalent light reflection anomalies. Images with defects also tend to be brighter on average. That can sometimes give the network the impression that there is a correlation between image brightness and the presence of damage. Similarly, most FN images are darker because images without damage tend to be darker. Some examples of this can be

seen in Figure 6. For future work, a more in-depth pre-processing can be performed on images to ensure that the influence of the brightness is minimised across the entire image dataset.

Table 2: Evaluation metrics for two different tasks

Task	1	2
Accuracy	96.2%	86.25%
Precision	100%	91.3%
Recall	93.62%	85.71%
F-1	96.7%	88.42%

Table 3: Average training time of each task

Task	1	2
Training Time	1h 2m 2s	42m 7s

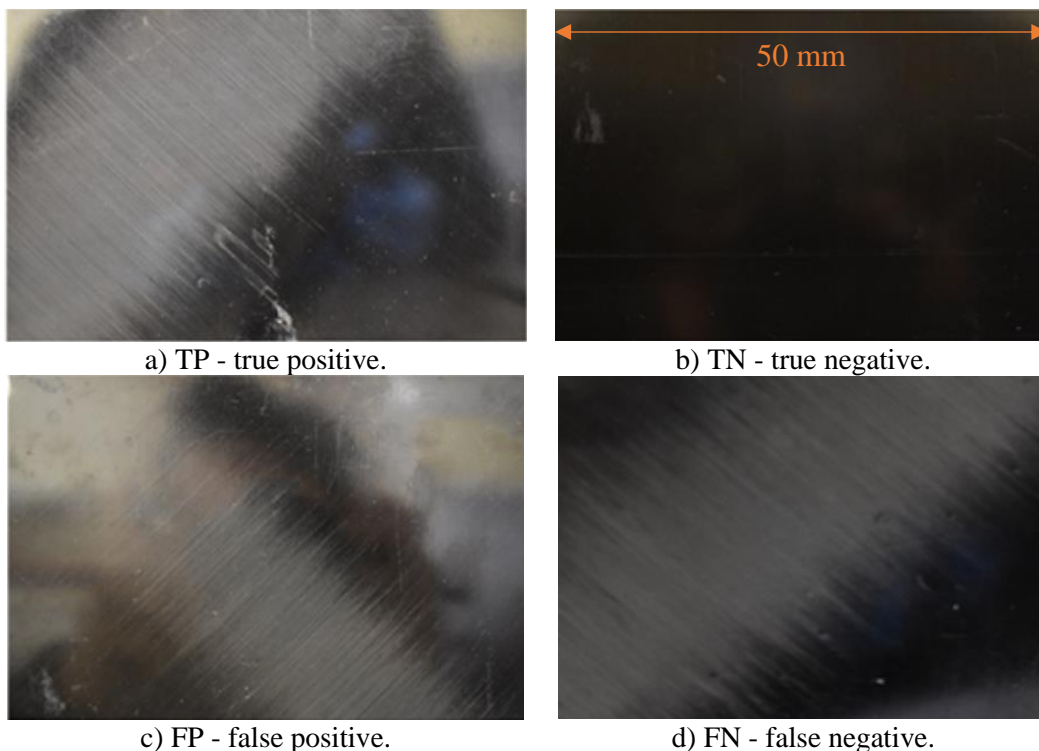


Figure 6: Some examples of the predictions that are most prevalent across the network.

## CONCLUSIONS

This research successfully applied ResNet to detect BVID on both impacted and non-impacted surfaces of FRP composite panels. The input to the DL model was simple surface images; thus, this study proposed an autonomous BVID recognition system in FRP composite materials using a DL model. It was concluded that the AI-based BVID detection accuracy is higher on the back-face than the front-face. This is due to a more recognisable damage pattern on the back-face of panels investigated in this study. Therefore, where the non-impacted side of the structure is accessible, using back-face images as input to an AI network is preferred. Further analysis of the results also highlighted the key role that light reflection can have on the accuracy of an AI-based predictive model.

## REFERENCES

Deng, J., Dong, W., Socher, R., Li, L.-J., Kai Li, & Li Fei-Fei. (2009). ImageNet: A large-scale hierarchical image database. *IEEE Conference on Computer Vision and Pattern Recognition*, 248–255. doi: 10.1109/cvpr.2009.5206848

- Deng, K., Liu, H., Yang, L., Addepalli, S., & Zhao, Y. (2023). Classification of barely visible impact damage in composite laminates using deep learning and pulsed thermographic inspection. *Neural Computing and Applications*, 1–15. doi: 10.1007/s00521-023-08293-7
- Fotouhi, M., Pui, W., Fotouhi, S., Jalalvand, M., & Wisnom, M. R. (2021). Detection of Barely Visible Impact Damage Using a Smart Hybrid Composite Surface Layer. *Twenty-Third International Conference on Composite Materials (ICCM23)*. Retrieved from <https://eprints.gla.ac.uk/234772/>
- Hasebe, S., Higuchi, R., Yokozeki, T., & Takeda, S. (2022a). Multi-task learning application for predicting impact damage-related information using surface profiles of CFRP laminates. *Composites Science and Technology*, 231(September 2022), 109820. doi: 10.1016/j.compscitech.2022.109820
- Hasebe, S., Higuchi, R., Yokozeki, T., & Takeda, S. (2022b). Internal low-velocity impact damage prediction in CFRP laminates using surface profiles and machine learning. *Composites Part B: Engineering*, 237(March), 109844. doi: 10.1016/j.compositesb.2022.109844
- He, K., Zhang, X., Ren, S., & Sun, J. (2016). Deep Residual Learning for Image Recognition. *Proceedings of the IEEE Conference on Computer Vision and Pattern Recognition (CVPR)*, 770–778. Retrieved from <http://image-net.org/challenges/LSVRC/2015/>
- Jung, K. C., & Chang, S. H. (2021). Advanced deep learning model-based impact characterization method for composite laminates. *Composites Science and Technology*, 207(December 2020), 108713. doi: 10.1016/j.compscitech.2021.108713
- Paszke, A., Gross, S., Massa, F., Lerer, A., Bradbury Google, J., Chanan, G., Killeen, T., Lin, Z., Gimelshein, N., Antiga, L., Desmaison, A., Xamla, A. K., Yang, E., Devito, Z., Raison Nabla, M., Tejani, A., Chilamkurthy, S., Ai, Q., Steiner, B., Chintala, S. (2019). PyTorch: An Imperative Style, High-Performance Deep Learning Library. *Advances in Neural Information Processing Systems*, 32.

#### **ACKNOWLEDGEMENT**

The authors acknowledge the financial support from SENAI Institute of Innovation in Polymer Engineering. The support from the University of Glasgow, Radboud University and Delft University of Technology are acknowledge as well.

#### **CONFLICT OF INTEREST**

The authors declare that they have no conflicts of interest associated with the work presented in this paper.

#### **DATA AVAILABILITY**

Data on which this paper is based is available from the authors upon reasonable request.